The Monte Carlo Method: Versatility Unbounded in a Dynamic Computing World
Chattanooga, Tennessee, April 17-21, 2005, on CD-ROM, American Nuclear Society, LaGrange Park, IL (2005)

THE NEUTRON_HP NEUTRON TRANSPORT CODE.

J.P. Wellisch
CERN
1211 Geneva 23, Switzerland
hpw@geant4.com

ABSTRACT

Simulation of low energy neutron interactions has been a field of strong activity for many years. In particle physics, it gains its particular importance from its use in radiation studies and activation, but also from the necessity to predict and simulate the background rates in the detector systems of the large collider or dark matter search experiments.

The effort described here targets the problems of neutron interactions for radiation transport in large detectors. The package is based on the Object Oriented paradigm, and is implemented in C++. It is a client of the geant4 hadronic implementation frameworks, and can be inter-operated with any of the other hadronic shower simulation components complying with this protocol. Models are provided for fission, capture, elastic, and inelastic scattering including absorption. The modelling is data driven. The data currently utilised are derived evaluations of ENDF-B, JENDL, BROND, CENDL, and others. The neutron scattering data formats used are originally based on the ENDF-B VI data format documentation, but have been evolved to enable easier maintenance and updaates of data.

Key Words: Monte Carlo, thermalization, neutron, dosimetry

1 INTRODUCTION

The neutron transport class library, neutron_hp, described here simulates the interaction of neutrons with kinetic energies from thermal energies up to O(20 MeV). Detailed modeling of this type of interactions is important in a fairly wide range of problems related to particle and nuclear physics, but also in military and medicial applications. Examples are neutron back-grounds in the LHC detectors, activation, single event upsets, backgrounds in Dark Matter searches, etc., but also neutron therapy, and land-mine search.

The code is fully integrated in the implementation frameworks of the geant4 hadronic physics (GHAD) code, and currently released with the geant4 source tree for conveniance of the user. The upper limit in neutron energy is set by the comprehensive evaluated neutron scattering data library, G4NDL, that the simulation is based on. The result of the code is doppler-broadened cross-section, or a set of secondary particles that can be passed on directly to the tracking sub-system of GEANT4 for further geometric tracking.

The model complies with the interface for use with the GEANT4 hadronic processes which enables their transparent use within the GEANT4 tool-kit together with all other GHAD compliant hadronic interaction models and cross-sections.

The interactions of neutrons at low energies are split into four parts to ensure consistancy with the other hadronic codes in GEANT4. We consider radiative capture, elastic scattering, fission, and inelastic scattering separately.

2 PHYSICS AND VERIFICATION

2.1 Inclusive Cross-sections

The cross-section data in G4NDL, the neutron data library used with the neutron_hp code, are not original evaluations, but are simply collected from a number of evaluated data libraries, and reformatted for the purpose of neutron_hp. These original data libraries are, in alphabtic order, Brond-2.1[5], CENDL-2.2[4], EFF-3[6], ENDF/B-VI.0[1], ENDF/B-VI.1, ENDF/B-VI.5, FENDL/MC-2.0[7], Jef-2.2[8], JENDL-FF[2], JENDL-3.1, JENDL-3.2, and MENDL-2[9]. The initial selection was guided by the FENDL criteria. It has undergone much evolution in recent years based on intercomparisons between the available evaluations, with a tendency to drive towards isotope wise data.

All cross-sections, for both inclusive and exlusive channels, are treated as point-wise cross-sections for reasons of accuracy of the physics. This way, for example accurate values for recoil energy distributions in elastic scattering can be obtained, something that is not available in many multi-group codes. Data from the evaluated data library have been processed, to explicitly include all neutron nuclear resonances in the form of point-like cross-sections rather than in the form of parametrisations. The resulting data have been transformed into a linearly interpolable format, such that the error due to linear interpolation between adjacent data points is smaller than 1 percent.

It is worth noting, that the inelastic cross-section definition in GEANT4 is not the same as the definition of inelastic cross-section in ENDF/B. Hence careful resumming of channels was needed in preparing the neutron scattering data for neutron_hp.

The inclusive cross-sections comply with the cross-sections data set interface of the GHAD framework. They are, when registered with the GEANT4 tool-kit at initialisation, used to select the basic process. In the case of fission and inelastic scattering, point-wise exclusive or semi-inclusive cross-sections are also used in order to decide on the active channel for an individual interaction. As an example, in the case of fission this could be first, second, third, or forth chance fission.

The data provided in the G4NDL database are zero Kelvin data, but no pre-processing is needed to bring them to the temperature of the materials in the problem. The temperature information from the detctor description is used at run-time, to doppler-broaden the cross-sections on the fly. We assume a free gas model for the motion of the nuclei in the material, and use a Monte Carlo integration technique to perform doppler broadening to the temperature of the local medium at the energy of the scattering neutron. Effects of molecular binding are not taken published, disabling the use of the distributed code in situations requiring accurate description of neutron moderators.

In figure1, we show the result for the neutron capture cross-section on Plutonium at several temperatures. The material, energies, and temperatures have been chosen to miror the standard BROADR @@@@ verification plot.

2.2 Elastic Scattering

The final state of elastic scattering is described by sampling the differential scattering cross-sections $\frac{\mathrm{d}\sigma}{\mathrm{d}\Omega}$. Two representations are supported for the normalised differential elastic scattering cross-section. The first is a tabulation of the differential cross-section, as a function of the cosine of the scattering angle θ and the kinetic energy E of the incoming neutron.

$$\frac{\mathrm{d}\sigma}{\mathrm{d}\Omega} \;=\; \frac{\mathrm{d}\sigma}{\mathrm{d}\Omega}\left(\cos\theta,\; E\right)$$

The tabulations used are normalised by $\sigma/(2\pi)$ so the integral of the differential cross-sections over the scattering angle yields unity.

In the second representation, the normalised differencial cross-section is represented as a series of legendre polynomials $P_l(\cos\theta)$, and the legendre coefficients a_l are tabulated as a function of the incoming energy of the neutron.

$$\frac{2\pi}{\sigma(E)}\frac{\mathrm{d}\sigma}{\mathrm{d}\Omega}\left(\cos\theta,\; E\right) \;=\; \sum_{l=0}^{n_l}\frac{2l+1}{2}a_l(E)P_l(\cos\theta)$$

As an example of the result, we show in figure2 for the elastic scattering of 15 MeV neutrons off Uranium a comparison of the simulated angular distribution of the scattered neutrons with evaluated data. The points are the evaluated data, the histogram is the Monte Carlo prediction.

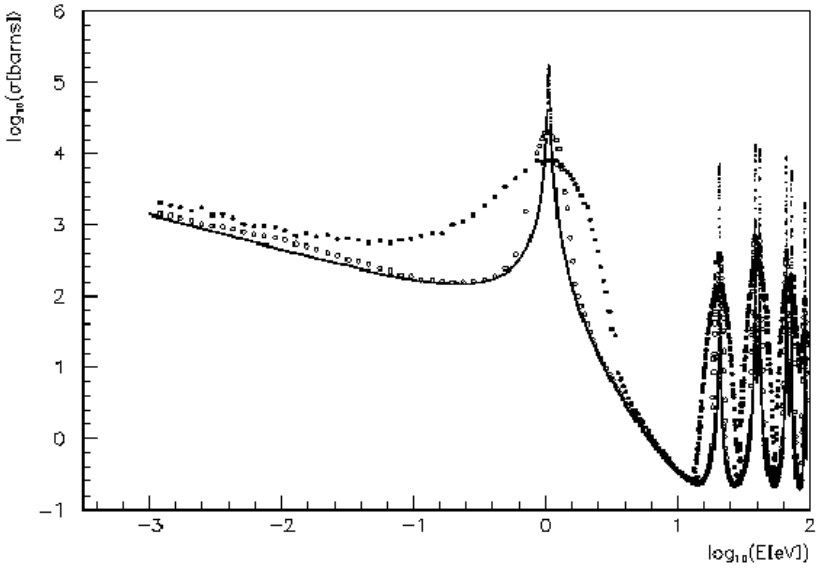

Figure 1: neutron capture cross-section on Plutonium at several temperatures. The material, energies, and temperatures have been chosen to miror the standard BROADR verification plot.

In order to provide full test-coverage for the algorithms, similar tests have been performed for $^{72}\mathrm{Ge}$, $^{126}\mathrm{Sn}$, $^{238}\mathrm{U}$, $^{4}\mathrm{He}$, and $^{27}\mathrm{Al}$ for a set of neutron kinetic energies. The agreement is very good for all values of scattering angle and neutron energy investigated.

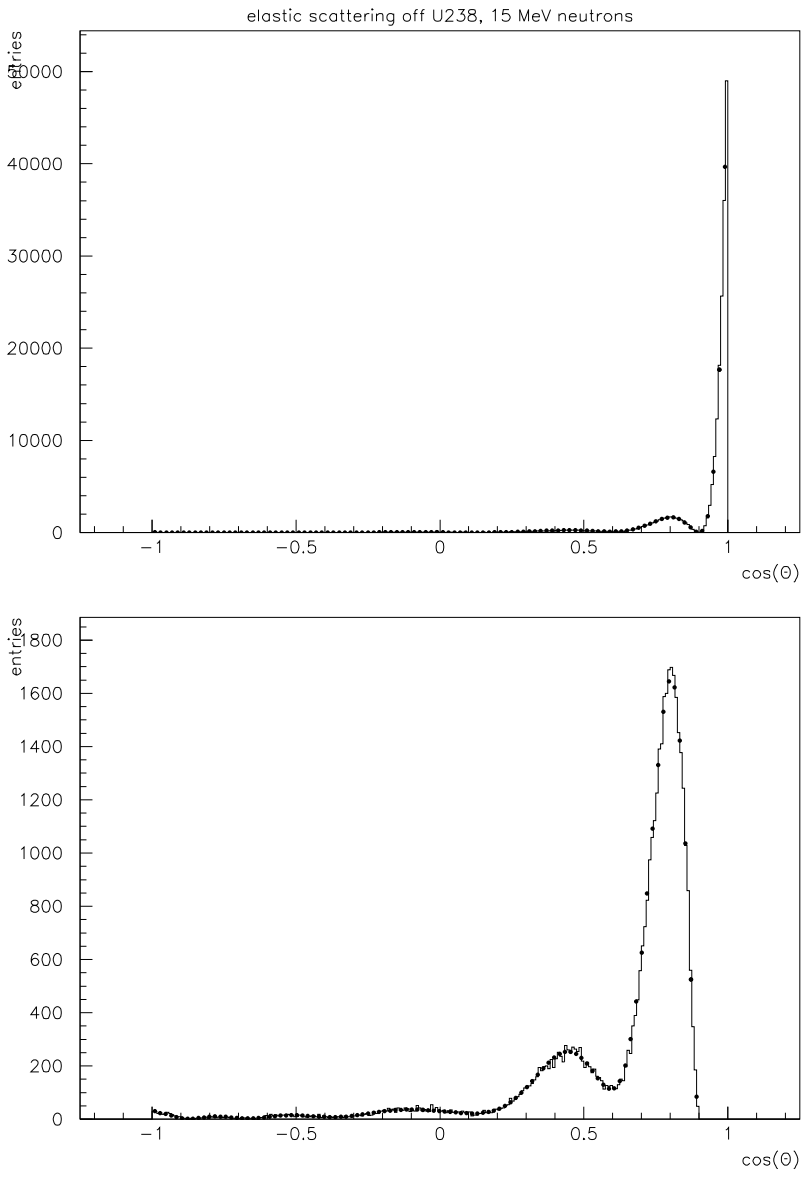

Figure 2: Comparison of data and Monte Carlo for the angular distribution of 15 MeV neutrons scattered elastically off Uranium (^{238}U). The points are evaluated data, and the histogram is the Monte Carlo prediction. The lower plot excludes the forward peak, to better show the Frenel structure of the angular distribution of the scattered neutron.

2.3 Radiative Capture

The final state of radiative capture is described by either photon multiplicities, or photon production cross-sections, and the discrete and continuous contributions to the photon energy spectra, along with the angular distributions of the emitted photons.

For the description of the photon multiplicity there are two supported data representations. It can either be tabulated as a function of the energy of the incoming neutron for each discrete photon as well as the eventual continuum contribution, or the full transition probability array is known, and used to determine the photon yields. If photon production cross-sections are used, only a tabulated form is supported.

The photon energies E_γ are associated to the multiplicities or the cross-sections for all discrete photon emissions. For the continuum contribution, the normalised emission probability f is broken down into a weighted sum of normalised distributions g.

$$f\left(E \rightarrow E_\gamma\right) \;=\; \sum_i p_i(E) g_i(E \rightarrow E_\gamma)$$

The weights p_i are tabulated as a function of the energy E of the incoming neutron. For each neutron energy, the distributions g are tabulated as a function of the photon energy. As in the ENDF/B-VI data formats[1], several interpolation laws are used to minimise the amount of data, and optimise the descriptive power. All data are derived from evaluated data libraries.

The techniques used to describe and sample the angular distributions are identical to the case of elastic scattering, with the difference that there is either a tabulation or a set of legendre coefficients for each photon energy and continuum distribution.

As an example of the results we show in figure3 the energy spectrum of the emitted photons for the radiative capture of 14 MeV neutrons on Uranium (^{238}U). Similar comparisons for photon yields, energy and angular distributions have been performed for capture on $^{238}\mathrm{U}$, $^{235}\mathrm{U}$, $^{23}\mathrm{Na}$, and $^{14}\mathrm{N}$ for a set of incoming neutron energies. In all cases investigated the agreement between evaluated data and Monte Carlo is very good.

2.4 Fission

For neutron induced fission, we take first chance, second chance, third chance and forth chance fission into account.

Neutron yields are tabulated as a function of both the incoming and outgoing neutron energy. The neutron angular distributions are either tabulated, or represented in terms of an expansion in legendre polynomials, similar to the angular distributions for neutron elastic scattering. In case no data are available on the angular distribution, isotropic emission in the centre of mass system of the collision is assumed.

There are six different possibilities implemented to represent the neutron energy distributions. The energy distribution of the fission neutrons $f(E \rightarrow E')$ can be tabulated as a normalised function of the incoming and outgoing neutron energy, again using the ENDF/B-VI interpolation schemes to minimise data volume and maximise precision.

The energy distribution can also be represented as a general evaporation spectrum,

$$f(E \rightarrow E') \; = \; f\left(E'/\Theta(E)\right).$$

Here E is the energy of the incoming neutron, E' is the energy of a fi ssion neutron, and $\Theta(E)$ is effective temperature used to characterise the secondary neutron energy distribution. Both the effective temperature and the functional behaviour of the energy distribution are taken from tabulations.

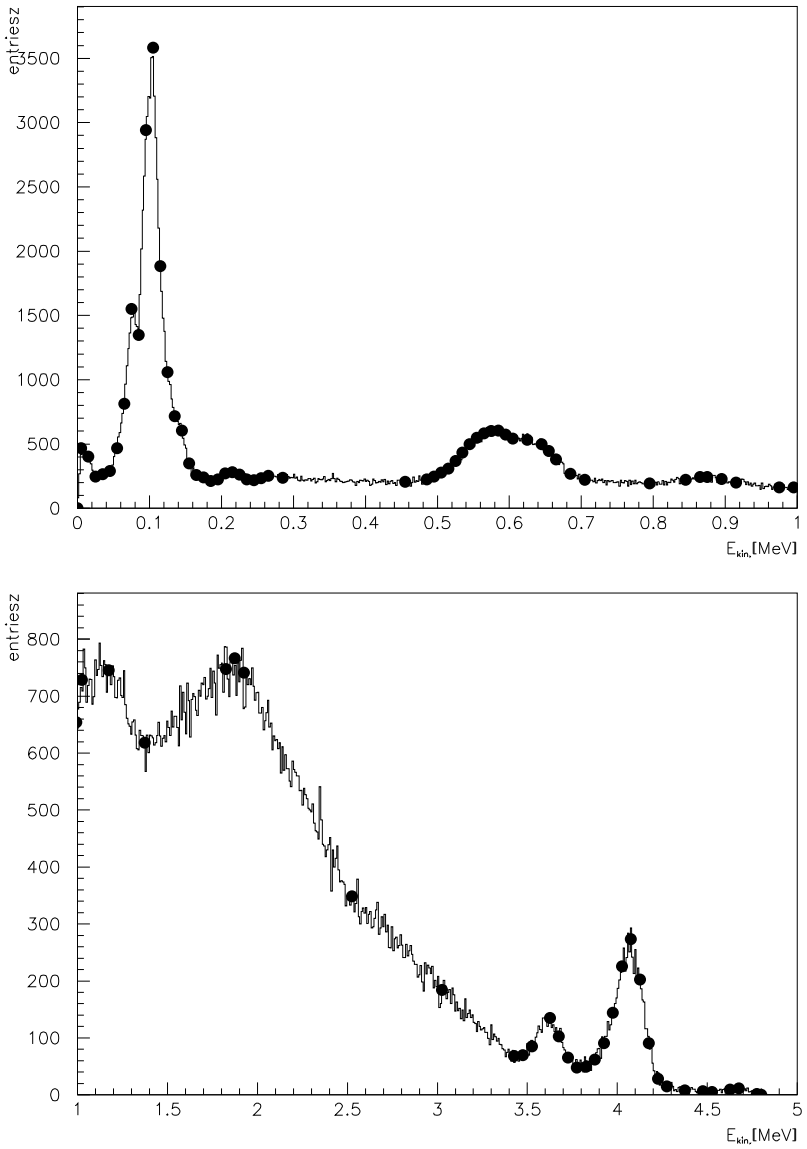

Figure 3: Comparison of data and Monte Carlo for photon energy distributions for radiative capture of 15 MeV neutrons on Uranium (^{238}U). The points are evaluated data, the histogram is the Monte Carlo prediction.

Alternatively energy distribution can be represented as a Maxwell spectrum,

$$f(E \rightarrow E') \ \propto \ \sqrt{E'} \mathrm{e}^{E'/\Theta(E)},$$

or a evaporation spectrum

$$f(E \rightarrow E') \ \propto \ E' \mathrm{e}^{E'/\Theta(E)}.$$

In both these cases, the effective temperature is tabulated as a function of the incoming neutron energy.

The last two options are the energy dependent Watt spectrum, and the Madland Nix spectrum. For the energy dependent Watt spectrum, the energy distribution is represented as

$$f(E \rightarrow E') \ \propto \ \mathrm{e}^{-E'/a(E)} \sinh \sqrt{b(E)E'}.$$

Here both the parameters a, and b are used from tabulation as function of the incoming neutron energy. In the case of the Madland Nix spectrum, the energy distribution is described as

$$f(E \rightarrow E') \ = \ \frac{1}{2} \left[g(E', < K_l >) \ + \ g(E', < K_h >) \right].$$

Here

$$g(E', < K >) \ = \ \frac{1}{3\sqrt{< K > \Theta}} \left[u_2^{3/2} E_1(u_2) - u_1^{3/2} E_1(u_1) + \gamma(3/2, u_2) - \gamma(3/2, u_1) \right],$$

$$u_1(E', < K >) = \frac{(\sqrt{E'} - \sqrt{< K >})^2}{\Theta}, \text{ and}$$

$$u_2(E', < K >) = \frac{(\sqrt{E'} + \sqrt{< K >})^2}{\Theta}.$$

Here K_l is the kinetic energy of light fragments and K_h the kinetic energy of heavy fragments, $E_1(x)$ is the exponential integral, and $\gamma(x)$ is the incomplete gamma function. The mean kinetic energies for light and heavy fragments are assumed to be energy independent. The temperature Θ is tabulated as a function of the kinetic energy of the incoming neutron.

Fission photons are describes in analogy to capture photons, where evaluated data are available. The measured nuclear excitation levels and transition probabilities are used otherwise, if available.

As an example of the results is shown in figure 4 the energy distribution of the fission neutrons in third chance fission of 15 MeV neutrons on Uranium (^{238}U). This distribution contains two evaporation spectra and one Watt spectrum. Similar comparisons for neutron yields, energy and angular distributions, and well as fission photon yields, energy and angular distributions have been performed for ^{238}U, ^{235}U, ^{234}U, and ^{241}Am for a set of incoming neutron energies. In all cases the agreement between evaluated data and Monte Carlo is very good.

The simulation of fission fragment distributions is not included, a circumstance, which was a mandated constraint on our work.

2.5 Inelastic Scattering

For inelastic scattering, the currently supported final states are (nA→) nγs (discrete and continuum), np, nd, nt, n^{3}He, nα, nd2α, nt2α, n2p, n2α, npα, n3α, 2n, 2np, 2nd, 2nα, 2n2α, nX, 3n, 3np, 3nα, 4n, p, pd, pα, 2p d, dα, d2α, dt, t, t2α, ^{3}He, α, 2α, and 3α.

The photon distributions are again described as in the case of radiative capture.

The possibility to describe the angular and energy distributions of the final state particles as in the case of fission is maintained, except that normally only tabulation of secondary energies is applicable.

In addition, we support the possibility to describe the energy angular correlations explicitly, in analogy with the ENDF/B-VI data formats. In this case, the production cross-section for reaction product n can be written as

$$\sigma_n(E, E', \cos(\theta)) \; = \; \sigma(E) Y_n(E) p(E, E', \cos(\theta)).$$

Here $Y_n(E)$ is the product multiplicity, $\sigma(E)$ is the inelastic cross-section, and $p(E, E', \cos(\theta))$ is the distribution probability. Azimuthal symmetry is assumed.

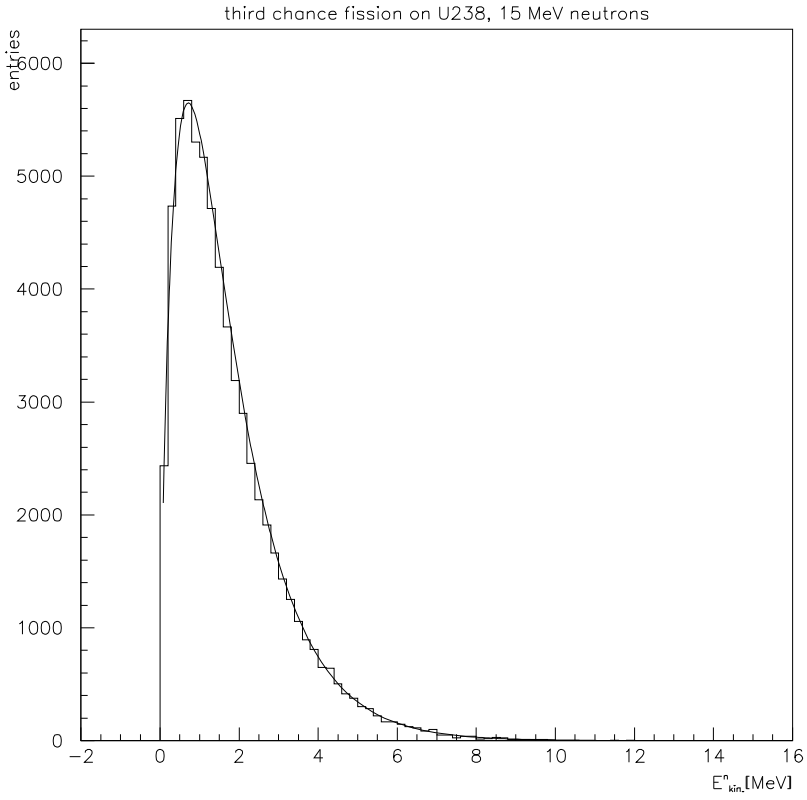

Figure 4: Comparison of data and Monte Carlo for fission neutron energy distributions for induced fission by 15 MeV neutrons on Uranium (^{238}U). The curve represents evaluated data and the histogram is the Monte Carlo prediction.

The representations for the distribution probability supported are isotropic emission, discrete two-body kinematics, N-body phase-space distribution, continuum energy-angle distributions, and continuum angle-energy distributions in the laboratory system.

The description of isotropic emission and discrete two-body kinematics is possible without further information. In the case of N-body phase-space distribution, tabulated values for the number of particles being treated by the law, and the total mass of these particles are used. For the continuum energy-angle distributions, several options for representing the angular dependence are available. Apart from the already introduced methods of expansion in terms of legendre polynomials, and tabulation (here in both the incoming neutron energy, and the secondary energy), the Kalbach-Mann systematic is available. In the case of the continuum angle-energy distributions in the laboratory system, the tabulated form in incoming neutron energy, product energy, and product angle is available.

Detailed comparisons for product yields, energy, and angular distributions have been performed for a set of incoming neutron energies, to achieve close to full test coverage. In all cases investigated, the agreement between evaluated data and Monte Carlo is very good.

3 SUMMARY

We have provided a neutron transport code for the GHAD tool-kit, and a data library that allows to use the code with other models consistent with the GHAD abstract interfaces.

By way of abstraction and code reuse we minimised the amount of code to be written and maintained. The concept of self-sampling containers lead to abstraction and encapsulation of data representation and the corresponding random number generators. The Object Oriented design allows for easy extension of the cross-section base of the system.

It is a data driven model, and covers the energy range from thermal neutron eneries up to 20 MeV. It uses point-wise cross-section data. The doppler-broadening is done on the fly, thus avoiding pre-formatting of neutron scattering data by the user, and making the simulation of neutron transport problems easily acessible to a large number of applications and users.

4 REFERENCES

1. ENDF/B-VI: Cross Section Evaluation Working Group, *ENDF/B-VI Summary Document*, Report **BNL-NCS-17541 (ENDF-201)** (1991), edited by P.F. Rose, National Nuclear Data Center, Brookhave National Laboratory, Upton, NY, USA.
2. JENDL-3: T. Nakagawa, et al., *Japanese Evaluated Nuclear Data Library, Version 3, Revision 2,* **J. Nucl. Sci. Technol. 32**, 1259 (1995).
3. Jef-2: C. Nordborg, M. Salvatores, *Status of the JEF Evaluated Data Library*, **Nuclear Data for Science and Technology**, edited by J. K. Dickens (American Nuclear Society, LaGrange, IL, 1994).
4. CENDL-2: Chinese Nuclear Data Center, *CENDL-2, The Chinese Evaluated Nuclear Data Library for Neutron Reaction Data*, Report **IAEA-NDS-61**, Rev. 3 (1996), International Atomic Energy Agency, Vienna, Austria.

5. Brond-2.2: A.I Blokhin et al., *Current status of Russian Nuclear Data Libraries*, **Nuclear Data for Science and Technology**, Volume2, p.695. edited by J. K. Dickens (American Nuclear Society, LaGrange, IL, 1994)
6. H.D. Lemme, EFF-2.4, The European Fusion File 1994, including revisions up to May 1995, Summary Documentation, IAEA-NDS-170 (1995)
7. ”FENDL/MC-2.0, The processed cross-section libraries for neutron-photon transport calculations, version 1 of February 1998”. Summary documentation H. Wienke and M. Herman, report IAEA-NDS-176 Rev. 0 (International Atomic Energy Agency, April 1998).
8. C. Nordborg, M. Salvatores, ”Status of the JEF Evaluated Data Library”, Proceedings of the International Conference on Nuclear Data for Science and Technology, Gatlinburg 1994, p680.
9. Yu.N. Shubin, V.P. Lunev, A.Yu. Konobeyev, A.I. Ditjuk, ”Cross section data library MENDL-2 to study activation as transmutation of materials irradiated by nucleons of intermediate energies”, report INDC(CCP)-385 (International Atomic Energy Agency, May 1995).